High-definition OBN seismic processing to enhance the interpretability of sand intrusions in the Balder-Ringhorne area

F. Buriola[1], J. Rokke[2], S. Høgden[2], M. Gelhaus[2], M. Trulsvik[3]

[1] Viridien; [2] Vår Energi; [3] TGS

Summary

The main reservoirs in the Balder and Ringhorne areas consist of large Paleocene sand mounds as well as Eocene sands, including thin and steeply dipping injectite bodies. Imaging of the targets in the legacy towed-streamer data is challenging due to sub-optimal signal-to-noise ratio, kinematic distortions caused by the complex overburden, and limited illumination provided by the narrow-azimuth surveys. Recent acquisition of the dense Heimdal Terrace OBN survey provided access to full azimuth, longer offsets, and higher trace density. Through state-of-the-art processing of the up-going wavefield and high-frequency velocity model building in conjunction with better illumination from the OBN data, a significant uplift was achieved in AVO attributes and structural imaging, with less wave-fronting noise that obscured the mapping of targets in the legacy data. In the near surface, the shallow illumination was further expanded by joint primary and multiple imaging, to enhance lateral and vertical resolution and reduce the acquisition footprint to a negligible level.

High-definition OBN seismic processing to enhance the interpretability of sand intrusions in the Balder-Ringhorne area

Introduction

The Heimdal Terrace ocean bottom node (OBN) survey, located in the Viking Graben in the Norwegian North Sea, is the second survey acquired as part of a large-scale multi-client programme that also includes the Utsira (2018 - 2019) and Sleipner (2023) dense OBN surveys (Figure 1a). Nodes from the three surveys cover a combined area of 3,705 km^2, using approximately 250,000 unique receiver positions, forming the largest continuous OBN dataset in the North Sea to date.

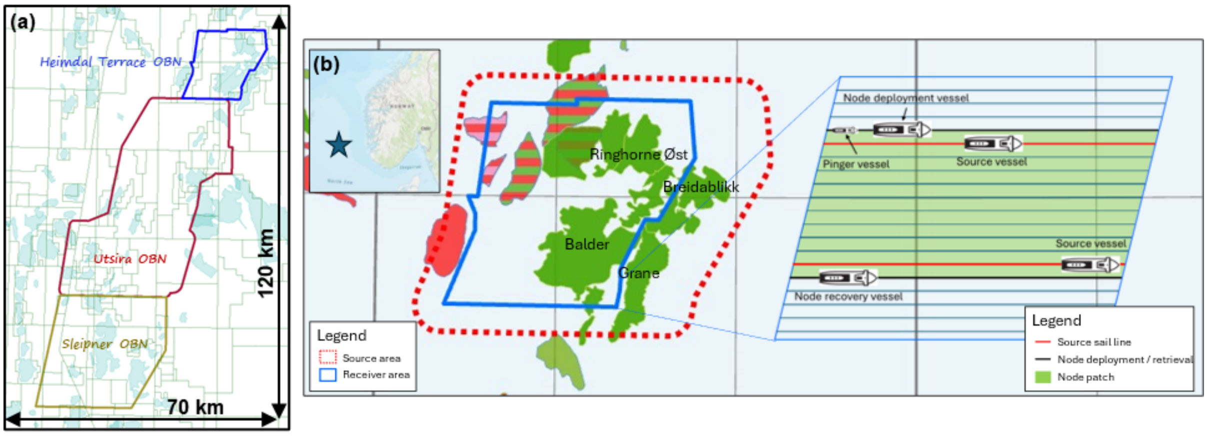

Figure 1 *(a) Location map showing Heimdal Terrace (blue polygon), Utsira (red) and Sleipner (green) OBN surveys, acquired as part of a large multi-client OBN programme between 2018 and 2023. (b) Map showing node (blue polygon) and source (red polygon) areas for Heimdal Terrace OBN. Vessel operations in the illustration to the right (Trulsvik et al., 2024).*

The Heimdal Terrace OBN, situated in water depths ranging from 100 to 134 m, covers a full-fold area of approximately 426 km^2 (Figure 1b). The receiver station interval is 50 m with a receiver line spacing of 300 m. A 3D source carpet was shot with multi-vessel, triple-source configuration with a shot interval of 25 m (nominal 8.33 m flip-to-flop-to-flap) and source line spacing of 50 m. This acquisition was designed to provide full-azimuth coverage, long offsets up to 32 km, and high trace density. The bulk of the nodes were deployed using nodes on a rope; 286 nodes were deployed by remotely operated vehicle vessels in proximity to surface and subsea obstructions. Acquisition completed in June 2023 with the final processed images delivered in 2024.

The Heimdal Terrace OBN survey covers the producing Balder and Ringhorne fields and the near-field exploration acreage to the west in the North Sea (Figure 1b). At the Balder field, the main reservoirs consist of large Paleocene sand mounds as well as interconnected, remobilised and injected Eocene sands. The complex overburden is characterised by near-surface channels, shallow localised gas pockets, and widespread v-brights (Huuse et al., 2004). These structures have a significant impact on the seismic image quality at the prospect level if the imaging velocity is not correctly resolved. Existing legacy narrow-azimuth towed-streamer data in the area show sub-optimal imaging quality at the target interval due to severe kinematic distortions and the presence of wave-fronting artefacts. These “smile”-like artefacts occur due to non-cancellation of energy during migration caused by recording aperture limitations perpendicular to the acquisition direction. They are predominant at and above the rugose chalk layer, located just below the steeply dipping injectites.

The main objective for processing of the newly acquired OBN data was to achieve higher signal bandwidth and improved event continuity over the available legacy towed-streamer data. In this abstract, we demonstrate how this objective was accomplished through state-of-the-art processing of the up-going wavefield and high-frequency velocity model building in conjunction with better illumination from the OBN data. This resulted in improved seismic images with increased confidence in the assessment of prospects.

Processing Highlights

To unlock the full potential of the OBN data and address the geophysical challenges, the OBN data was run through a comprehensive processing workflow including the latest model building technology.

To compensate for the kinematic distortions and amplitude loss from the shallow overburden, velocity and Q models need to be accurately estimated. The first round of velocity model building updated both models, derived by a joint Vp/Q least-squares full waveform inversion (FWI) utilising diving waves up to 9 Hz. This allows a joint update of the two models and reduced crosstalk between them in the inversion process. The update was kept down to around 2 km depth, where the high-velocity layer corresponding to the Shetland interval limits the penetration of diving waves even with 14 km offsets. Remaining high-wavenumber structural undulations were captured by visco-acoustic Time-lag FWI (Zhang et al., 2018) up to 25 Hz, utilising the full recorded wavefield including diving waves, ghosts, multiples and primary energy, to invert for high-frequency details at all depths. This led to a geologically and structurally coherent velocity update, with added high-frequency detail and velocity contrasts throughout, and high level of spatial delineation of the complex overburden (Figure 2c).

Processing was carried out on the up-going wavefield for reservoir imaging. The processing sequence applied standard data initialisation including repositioning, geophone rotation, sensor calibration, water layer and shot layback corrections. Due to the multi-vessel acquisition, deblending was also applied in the common-receiver domain. After data initialisation, shot regularisation to a 12.5 × 12.5 m grid with spatial anti-aliasing was applied. The hydrophone and geophone components were then calibrated. Following wavefield separation, the up-going and down-going wavefields were input to Up-Down Deconvolution. Guided noise attenuation using migration and subsequent demigration to form a noise-free model aided in improving the signal-to-noise levels in the data prior to imaging. Imaging was performed using Q-Kirchhoff pre-stack depth migration. A 60 Hz reverse time migration (RTM) was also implemented to better honour the velocity model complexity, combining individual vector offset outputs via a bespoke method based on a cross-correlation weighted stack scheme (Liu et al., 2009).

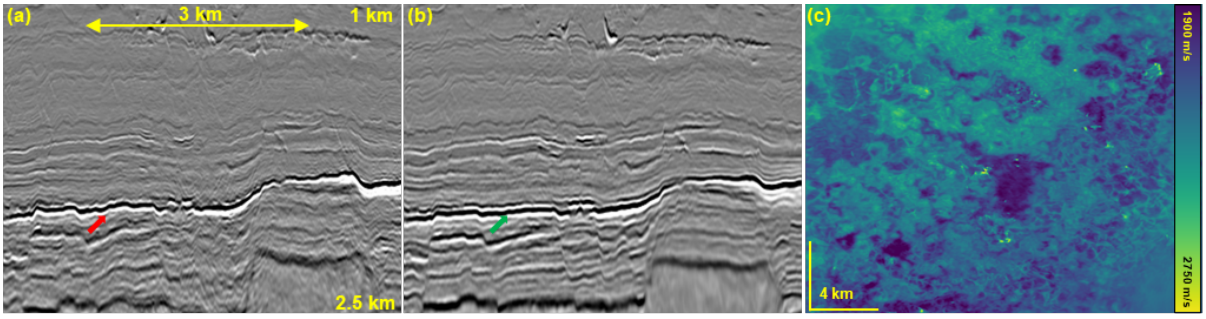

Figure 2 *(a) Legacy streamer Kirchhoff stack in depth; (b) 60 Hz RTM stack in depth of the OBN Up-Down deconvolution data; (c) Depth slice at 1200 m of the 25 Hz velocity model used to image the OBN data.*

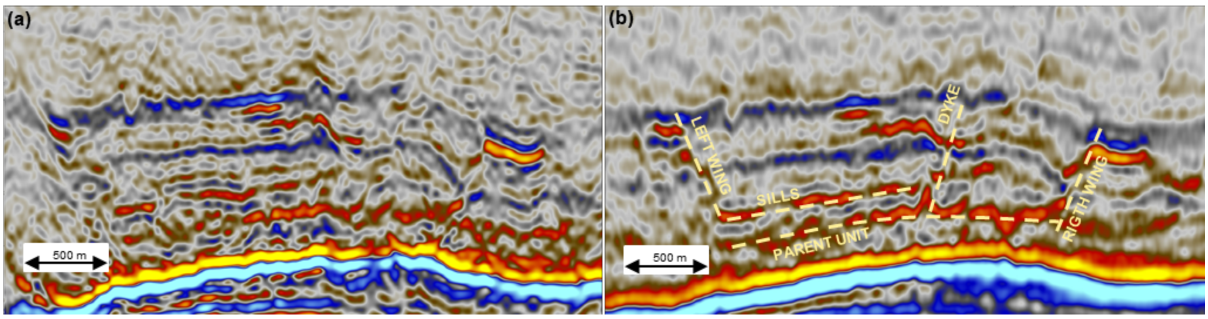

Figure 3 *(a) Legacy streamer Kirchhoff 27-33° stack; (b) Corresponding image for the OBN data, where the geometries of the sands are more recognizable due to reduced contamination from wave-fronting.*

The final 60 Hz RTM stack (Figure 2b) compares favourably to the Kirchhoff stack of the legacy streamer survey (Figure 2a) across many aspects. A profound improvement to structural imaging was realised from a combination of illumination, enhanced spectral content and a high-frequency detailed velocity model. This improvement brought greater reliability in interpretations of the Jurassic sediments below 1800 m and a reduction of short wavelength distortions at Top Shetland (red arrow in Figure 2a). At a reservoir scale, Figure 3a shows how wave-fronting noise hinders mapping of steeply dipping injectites and sills on the legacy streamer far-angle stack. This is much less prominent on the new OBN data (Figure 3b) where complex structures can be tracked with greater confidence, such as the saucer-shaped parent unit with sided wings/dikes as well as the sills located above the parent unit.

Rock physics analysis shows that sands present in the Balder area have a clear AVO behaviour. Oil bearing sands are identified based on near-to-far brightening, whereas water bearing sands display a class 1-2P AVO response. Negative gradient is therefore a powerful attribute for sand interpretation. Figures 4a and 4b show an example where the gradient impedance was used to interpret the top and base of the Hermod sand system, characterised by an AVO class 2P response. Reduction in short wavelength distortions at Top Shetland along with less wave-fronting artefacts in the new OBN data produced a more stable gradient attribute in terms of amplitude and signal-to-noise ratio, increasing the interpretability of prospects.

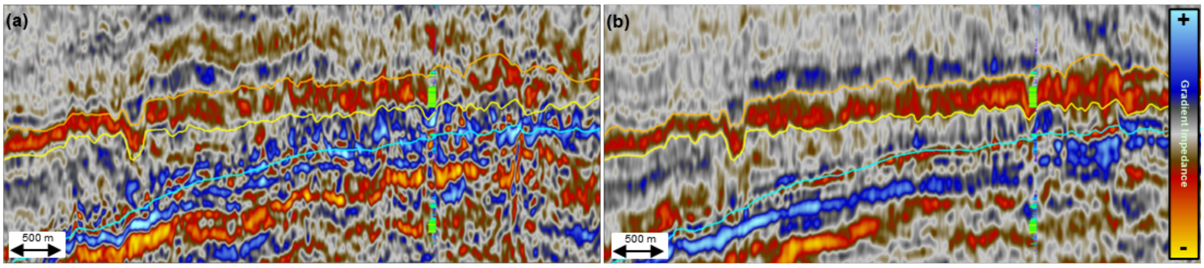

Figure 4 *(a) Gradient impedance computed from legacy streamer Kirchhoff data; (b) Corresponding image for the OBN data. Top (orange line) and base (yellow line) of the Hermod sand system are more trackable in the OBN data due to less contamination from wave-fronting generated at the Top Shetland reflector (cyan line). Porosity log is plotted along the well path.*

Joint Primary and Multiple Imaging

While OBN seismic benefits from full-azimuth coverage and very long offsets, receiver spacing is often considerably sparser than conventional towed-streamer acquisitions. This is also the case for the Heimdal Terrace survey, where the receiver spacing on a 50×300 m grid is too sparse for the imaging of shallow layers with primary reflections due to lack of small reflection angles away from the receiver lines (Figures 5a, 5b). Mirror migration of down-going data (Grion et al., 2007) is a potential solution to improve shallow illumination, but it is limited by only utilising the first order of multiples (the receiver ghost). A test of cascaded joint primary and multiple imaging (Poole and Farshad, 2024) was performed, which uses all the recorded data, including all orders of multiples (Figure 5c, 5d). In comparison to primary-only imaging, the cascaded primary and multiple imaging excels in resolution in the near shallow, better delineating small features and channels, with reduced acquisition footprint in the near surface and less wavelet stretching. The lateral and vertical resolution enhancement is significant over the legacy shallow imaging (Figures 5e, 5f).

Conclusions

Imaging of the Paleocene sand mounds, as well as injected Eocene sands in the Balder region, has historically been challenging due to the limitations of narrow-azimuth towed-streamer data. Recent acquisition of OBN data provided access to full-azimuth and longer offset data. Combined with bespoke processing of the up-going wavefield and imaging with a detailed velocity model, the new OBN data showed improvements in structural imaging and signal-to-noise ratio, cleaner AVO attributes and a significant reduction in wave-fronting artefacts compared to existing legacy towed-streamer data. Application of joint primary and multiple imaging allowed a further increase in illumination and resolution of the near surface.

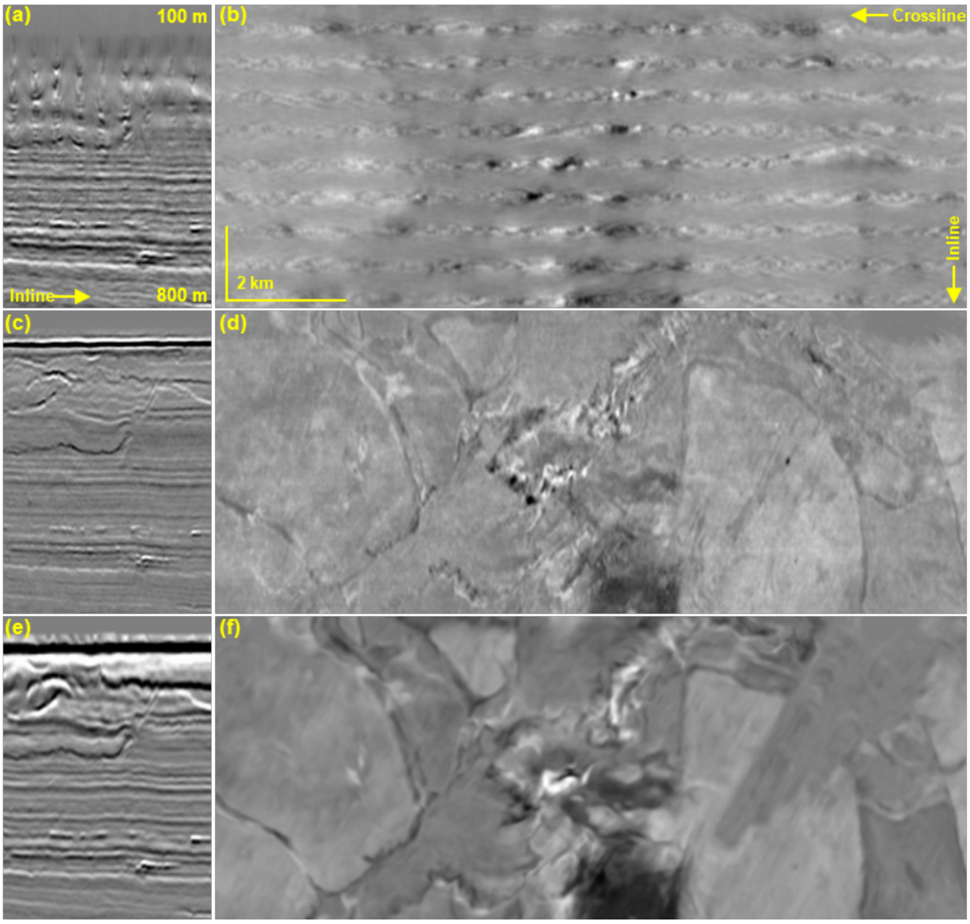

***Figure 5** (a) Q-Kirchhoff near surface crossline section of the OBN Up-Down deconvolution data and (b) time slice at 244 ms; (c, d) Corresponding images for cascaded joint primary and multiple imaging using OBN data; (e, f) Legacy streamer Kirchhoff stack.*

Acknowledgements

The authors acknowledge colleagues in Vår Energi, Viridien and TGS for their contribution and permission to publish this paper. Processing results courtesy of Viridien Subsurface Imaging. Colleagues from ENI (Dario Rosa and Francesco Lo Duca) are thanked for their fruitful discussions during processing, SAE for their contribution to the data acquisition, and Vår Energi ASA and Kistos Norway AS for permission to share data examples.

References

Grion, S., Exley, R., Manin, M., Miao, X-G., Pica, A., Wang, Y., Granger, P-Y. and Ronan, S. [2007] Mirror imaging of OBS data. *First Break*, **25**(11), 37-42.

Huuse, M., Duranti, D., Steinsland, N., Guargena, C., Prat, P., Holm, K., Cartwright, J. and Hurst, A. [2004] Seismic Characteristics of Large-Scale Sandstone Intrusions in the Paleogene of the South Viking Graben, UK and Norwegian North Sea. Geological Society, London, Memoirs, 29, 263–278.

Liu, G., Fomel, S., Lin, L. and Chen, X. [2009] Stacking seismic data using local correlation. *Geophysics*, **74**(3), 43-48.

Poole, G. and Farshad, M. [2024] Exploring the benefits and pitfalls of using multiples in imaging. *First Break*, **42**(12), 47-52.

Trulsvik, M., Burnie, I. and Bertrand, A. [2024] Acquisition of a Complex OBN survey in the Balder-Ringhorne area of the North Sea. *85th EAGE Annual Conference & Exhibition*, Extended Abstracts.

Zhang, Z., Mei, J., Lin, F., Huang, R. and Wang, P. [2018] Correcting for salt misinterpretation with full-waveform inversion. *88th SEG Annual International Meeting*, Expanded Abstracts, 1143-1147.